Synthesis of Fe_3O_4/PMMA Composite Latex Particles: Kinetic Modeling

Ping-Chieh Wang,[1] Wen-Yen Chiu,[1] Tai-Horng Young[2]

[1]*Department of Chemical Engineering, National Taiwan University, Taipei, Taiwan, Republic of China*
[2]*Institute of Biomedical Engineering, College of Medicine and College of Engineering, National Taiwan University, Taipei, Taiwan, Republic of China*

Received 30 December 2004; accepted 31 October 2005
DOI 10.1002/app.23754
Published online in Wiley InterScience (www.interscience.wiley.com).

ABSTRACT: In this work, a generalized mathematical model was developed to estimate the variation of particle concentration during the entire course of soapless emulsion polymerization of methyl methacrylate with ferrofluid. Two mechanisms for the nucleation and growth of particles throughout the polymerization reaction were discussed: Mechanism I – seeded polymerization; and Mechanism II – self-nucleation polymerization. Here, the self-nucleation included homogeneous nucleation and micelle nucleation. Coagulation between particles, which came from different nucleation mechanisms during the course of polymerization, was considered and included in this model. When appropriate parameters were selected, this model could be successfully used to interpret the variation of particle concentration during the entire reaction. Under different conditions, rate of polymerization, number of radicals in each particle, average molecular weight of polymers, and rate constant of termination were also calculated. All of them explained the experimental results quite well. © 2006 Wiley Periodicals, Inc. J Appl Polym Sci 100: 4925–4934, 2006

Key words: Fe_3O_4; PMMA; composite latex particle; nucleation mechanism; kinetic model

INTRODUCTION

Ionic and nonionic[1] emulsifiers are usually used as stabilizers in emulsion polymerization. Madaeni[2] prepared polystyrene latices by emulsion polymerization. Three types of surfactant, i.e., sodium dodecylbenzene sulfonate (anionic), Triton X-100 and Vulcastab LW (nonionic), and hexadecyltrimetyl ammonium bromide (cationic), were used. The micelle formation of the surfactants played the major role of particle nucleation.

Soapless emulsion polymerization has received more attention in recent decades because it provides advantages for the synthesis of monodisperse latex. In this type of system, ionized initiators stabilize polymer particles. Several particle nucleation mechanisms have been proposed for emulsifier free systems, which can be divided into two main categories:

1. Micellar-like nucleation: This was proposed by Goodall et al.,[3] Cox et al.,[4] Chen and Piirma,[5] and Vanderhoff.[6] As the oligomeric radicals in the aqueous phase reached critical length, several of them aggregated together to form a micellar-like primary particle and began nucleation.
2. Homogeneous nucleation: This was proposed by Priest,[7] Fitch and Tsai,[8,9] and Hansen and Ugelstad.[10–14] When above the critical chain, each growing oligomeric radical precipitated from the aqueous phase and became a primary particle.

Both the aforementioned nucleation mechanisms could reasonably describe the phenomena of particle nucleation in different soapless emulsion polymerization systems. The former applied if a hydrophobic monomer was used. The latter was more desirable if a hydrophilic monomer was chosen. According to the GPC analysis, Fitch and Tsai[8] found that the maximum degree of polymerization of poly(methyl methacrylate) (PMMA) oligomers in the aqueous phase was 66. This was accepted as the critical chain length of PMMA oligomers in particle nucleation. In homogeneous nucleation, primary particles are unstable because they do not have enough surface charge. These primary particles start to coagulate, and their sizes grow until they have enough charge density on their surfaces to stabilize themselves. Then, the particle concentration in the aqueous phase levels off until the end of the reaction.

In addition, seeded emulsion polymerization was proposed to be an effective way to control particle concentration and size over the course of polymeriza-

Correspondence to: W.Y. Chiu (ycchiu@ccms.ntu.edu.tw).
Contract grant sponsor: National Science Council, Taiwan, Republic of China; contract grant number: NSC-92–2216-E-002–009.

tion. In our previous work, Lee et al.[15–17] synthesized the poly(methyl methacrylate)–polystyrene (PMMA/PS) composite latex by the method of two-stage soapless emulsion polymerization. PMMA latex particles obtained from the first stage of polymerization acted as seeds, and the second stage of polymerization of styrene followed. The kinetic behavior of seeded polymerization was discussed in detail.

In this work, MMA emulsion polymerization was conducted in the presence of ferrofluid. A generalized kinetic model was proposed to simulate the particle nucleation and to interpret the variation of particle concentration, rate of polymerization, and average molecular weight of polymers during the entire course of polymerization.

THEORETICAL TREATMENT

According to our previous work,[18] two nucleation mechanisms were proposed as given later to explain the particle growth and the morphology of Fe_3O_4/PMMA particles at different experimental conditions Mechanism I–seeded nucleation. Ferrofluid acted as seeds. The primary particles generated from Mechanism I were Fe_3O_4 containing particles. Mechanism II –self-nucleation. It included homogeneous nucleation and micelle nucleation. The primary particles generated from Mechanism II were Fe_3O_4-free particles.

For the emulsion polymerization of MMA with potassium persulfate (KPS) as initiator in the presence of ferrofluid, particles could generate from ferrofluid seeds, or from precipitated PMMA oligomers in water, or from the accumulated micelle formation of lauric acid. In our system, seeded nucleation, homogeneous nucleation, and micelle nucleation were considered simultaneously. During polymerization, the particles grew and coagulated with each other until the polymer particles received enough surface charge to stabilize themselves.

Based on the aforementioned nucleation mechanisms, the following kinetic equations could be derived.

Concentration of polymer particles

Three kinetic equations [eqs. (1)–(3)] were used to simulate the concentration of polymer particles.

$$\frac{dN_1}{dx} = -\frac{k_f}{2}N_1^2 \tag{1}$$

$$\frac{dN_2}{dx} = \phi k_p M_w R_{\mathrm{jcr}}(u(x) - u(x - x_0)) - k_f N_1 N_2 - \frac{k_f}{2}N_2^2 + \varphi f(x) \tag{2}$$

$$N = N_1 + N_2 \tag{3}$$

where $u(x - x_0)$ represents a step function, i.e.,

$$u(x - x_0) = 1 \; x \geq x_0$$

$$u(x - x_0) = 0 \; x < x_0$$

Where N_1 is the concentration of composite polymer particles, i.e., particles containing Fe_3O_4; N_2 is the concentration of pure PMMA particles, i.e., particles not containing Fe_3O_4; N is the total concentration of polymer particles; x is the conversion; and k_f is the coagulation constant. Equation 1 represents the concentration change of N_1 through coagulation. According to the Smoluchowski's coagulation equation,[14] k_f can be written as[19]

$$k_f = k_{f0} \exp\left(\frac{-V_{\mathrm{toc}}}{kT}\right) \tag{4}$$

and V_{toc} is the total potential energy.[14] Assuming that there is a linear relationship between V_{toc} and conversion x, i.e., $V_{\mathrm{toc}} = ax + b$, then k_f can be expressed as

$$k_f = k_{f0} \exp\left(\frac{-(ax + b)}{kT}\right) \tag{5}$$

The first term in eq. (2) represents the homogeneous nucleation of MMA during the initial stage of polymerization when the growing oligomers of MMA in water reach their critical chain length, they precipitate from the aqueous phase and form primary particles. ϕ is a correction factor in the homogeneous nucleation. With the existence of ferrofluid, the growing oligomer radicals in water can be largely adsorbed by the ferrofluid, and so the probability of homogeneous nucleation decreased. $f(x)$ represents the micelle nucleation during the course of polymerization. When polymer particles grew and coagulated during polymerization, the surfactant desorbed from particles gradually accumulated to a critical concentration for micelles, and then micelle nucleation occurred in the reaction. φ is a factor to express the possibility of micelle nucleation at different experimental conditions.

In our previous work, M15 was formed almost purely through seeded nucleation. For this extreme case, only seeded polymerization was considered [eq. (1)]. For the pure PMMA system, only homogeneous nucleation [eq.(2) omitting $f(x)$] was considered in the calculation. All the other systems in this work considered both eqs. (1) and (2) to calculate N_1 and N_2. Reasonable parameters were used in the simulation as shown in Tables I and II.

TABLE I
Symbols, Ingredients and Conditions for the Synthesis of Composite Polymer Latex

Symbol	M15	M30 (*or1KPS or1FD*)	M45	0.5KPS	2KPS	0.5FD	2FD	Pure PMMA
Methyl methacrylate (MMA) (g)	15	30	45	30	30	30	30	30
Initiator ($K_2S_2O_8$) (g)	0.405	0.405	0.405	0.203	0.811	0.405	0.405	0.405
Deionized water (g)	650	650	650	650	650	700	550	750
Ferrofluid volume (mL)	100	100	100	100	100	50	200	0

N2; 80°C; stirring rate: 300 rpm; reaction time: 60 min.

Combined with k_f in eq. (5), the concentration of particles, N_1, N_2, and N with different conversion can be calculated numerically by solving eqs. (1)–(3).

Rate of polymerization

The rate of polymerization of MMA can be expressed as

$$R_p = [M]_0 \frac{dx}{dt} = k_p [M]_p \bar{n} N \tag{6}$$

where $[M]_0$ is the total initial amount of monomer charged per liter of aqueous phase; x is the conversion; $[M]_p$ represents the monomer concentration in polymer particles; N is the concentration of polymer particles in the water phase; and $\bar{n}$ expresses the average number of radicals per polymer particle. In eq. (6), R_p is obtained from the conversion–time curve. Furthermore, if the values of k_p, N, and $[M]_p$ are known, the variation of $\bar{n}$ with reaction time can be determined.

Volume of a swollen polymer particle

The definition of $[M]_p$ is as follows:

$$[M]_p = \frac{V_{\text{monomer}} \rho_m}{M_0 (V_{\text{polymer}} + V_{\text{monomer}})} \tag{7}$$

where V_{polymer} is the volume of polymer in a polymer particle; V_{monomer} is that of the monomer; ρ_m expresses the monomer density; and M_0 represents the molecular weight of monomer. Equation (7) can be rearranged as

$$V_{\text{monomer}} = \frac{[M]_p V_{\text{polymer}}}{\frac{\rho_m}{M_0} - [M]_p} \tag{8}$$

Using TEM measurement, the number average diameter of dry polymer particles ($\bar{D}$) was obtained. It was the diameter of one particle that contained no monomer. Substituting eq. (8) into (7) V_p can be expressed as

$$V_p = V_{\text{polymer}} + V_{\text{monomer}} = \left(1 + \frac{[M]_p}{\frac{\rho_m}{M_0} - [M]_p}\right) V_{\text{polymer}} \tag{9}$$

According to the aforementioned definition, V_{polymer} is expressed as

$$V_{\text{polymer}} = \frac{4}{3}\pi \left(\frac{\bar{D}}{2}\right)^3 \tag{10}$$

Under different experimental conditions, the variation of V_p during the reaction can be calculated using eqs. (9) and (10).

Average molecular weight of polymers and rate constant of termination

The number average molecular weight of polymer is approximately described as

TABLE II
Parameters Used in the Simulation

	T (353 K)	Reference
$N_1(0)$ [mol/L-H_2O]	3.1×10^{-7}	
$N_2(0)$ [mol/L-H_2O]	0	20
$k_p M_w R_{\text{jcr}}$ [mol/L-H_2O]	6.33×10^{-6}	19,20–22
k_{f0} [mol/L-H_2O]	5×10^8	19
X_0	0.01887	19
$f(x)$ [mol/L-H_2O]	$9 \times 10^{-8}x + 8.23 \times 10^{-8}x^2$	
$[M_p]$	$X < 0.25$, $[M_p] = 6.0$ (mol/L) $X \geq 0.25$, $[M_p] = 6.0(1-X)/(1-0.25)$ (mol/L)	20

TABLE III
Parameters Used in the Simulation at Different Experimental Conditions

Symbol	k_f	ϕ	φ
Pure PMMA	$5 \cdot 10^8\, e^{\left(\frac{-1.8\times10^{-13}x-5\times10^{-15}}{1.38\times10^{-16}\times353}\right)}$	1	0
M15	$3.5 \cdot 10^8\, e^{\left(\frac{-1.5\times10^{-11}x-4\times10^{-12}}{1.38\times10^{-16}\times353}\right)}$	0	0
M30 (*or*1*KPS or*1*FD*)	$3 \cdot 10^8\, e^{\left(\frac{-8\times10^{-13}x-3\times10^{-15}}{1.38\times10^{-16}\times353}\right)}$	0.1	1
2FD	$4 \cdot 10^8\, e^{\left(\frac{-5\times10^{-13}x-3\times10^{-15}}{1.38\times10^{-16}\times353}\right)}$	0.05	1
0.5KPS	$3.5 \cdot 10^8\, e^{\frac{-3.5\times10^{-13}x-3\times10^{-15}}{1.38\times10^{-16}\times353}}$	0.05	0.2
2KPS	$3 \cdot 10^8\, e^{\left(\frac{-9.5\times10^{-13}x-6\times10^{-15}}{1.38\times10^{-16}\times353}\right)}$	0.2	1

$$\overline{M_n} \cong M_0 \frac{R_p}{R_t} = M_0 \frac{R_p}{\frac{k_t}{V_p N_A N}(\bar{n}N)^2} \tag{11}$$

where R_t is the rate of formation of polymers; k_t is the rate constant of termination; V_p is the volume of a swollen polymer particle; and N_A is the Avogadro's number.

Combining particle concentration [eq. (3)], rate of polymerization [eq. (6)], the volume of a swollen polymer particle [eq. (9)], $\bar{n}$ [eq. (6)], and the experimental results of $\overline{M_n}$, the termination rate constant k_t varied with conversion can be estimated from eq. (11).

EXPERIMENT

Material

Methyl methacrylate (MMA) was distilled under a nitrogen atmosphere and reduced pressure prior to polymerization. The other materials were of analytical grade and used without further purification. Distilled and deionized water was used throughout the work.

Synthesis of Fe_3O_4/PMMA composite polymer latex

In our previous work, the Fe_3O_4/PMMA composite polymer latex was synthesized by the method of soapless emulsion polymerization of MMA in the presence of ferrofluid. The symbols, ingredients, and conditions of the polymerization are listed in Table III. The synthesis of composite polymer latex was carried out at 80°C under a nitrogen atmosphere. The stirring rate was controlled at 300 rpm. After reacting for 1 h, the polymerization was completed.

Conversion

During the emulsion polymerization, a sample of the emulsion latex was periodically taken out of the reactor, immediately poured into a chilled hydroquinone methanol solution, and immersed in an ice bath to quench the reaction. The precipitated latex was dried in an oven at 50°C until the loss of weight did not change.

The conversion of the emulsion polymerization was calculated as follows:

$$\text{Conversion} = \frac{W_2 - W_1 \times F\% \times S}{W_1 \times M_0\%} \tag{12}$$

where W_1 is the weight of the sample taken from the vessel; W_2 is the weight of dry composite polymers obtained from the taken sample; M_0% is the weight percentage of monomers (MMA) initially in the reaction mixture; F% is the volume percentage of the ferrofluid initially in the reaction mixture; and S is the solid content of the ferrofluid (g/mL).

Morphology and size of latex particles

The morphology of latex particles was observed under transmission electron microscopy (TEM). The particle size was measured from TEM photos by taking the average of 50 latex particles, where the number average diameter was considered. To improve the contrast of the images of TEM photos, the latex samples were stained with 1% phosphotungstate solution at room temperature for 2 min prior to the TEM experiments.

Particle concentration versus conversion

The concentration of latex particles (N) as a function of conversion was calculated from the average diameter of polymer particles measured by TEM [eq. (13)]. Two assumptions were made: (1) the volume is additive between Fe_3O_4 and PMMA, and (2) Fe_3O_4 nanoparticles were encapsulated in PMMA particles.

$$N = \frac{\frac{W_M x}{d_p} + \frac{W_{Fe_3O_4}}{d_{Fe_3O_4}}}{\frac{\pi}{6}\bar{D}^3} \tag{13}$$

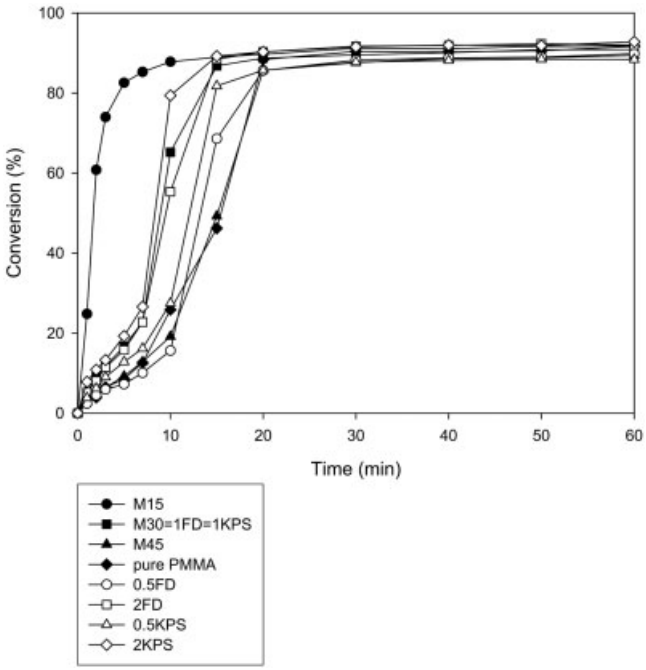

Figure 1 Conversion versus time of emulsion polymerization reaction at different monomer concentrations.

where W_M was the initial weight of monomer per liter of H_2O, x was the conversion of monomer, d_p was the density of polymer (1.19 g/cm^3), $W_{Fe_3O_4}$ was the weight of Fe_3O_4 per liter of H_2O, $d_{Fe_3O_4}$ was the density of Fe_3O_4 (5.12 g/cm^3), and $\bar{D}$ was the number average diameter of dry polymer particles measured by TEM.

Average molecular weight of polymers

The concentrated HCl (10 mL) was added in the sample of dried composite polymer (about 1 g) to remove Fe_3O_4 particles, and then toluene (10 mL) was used to extract the polymer. The extracted polymer was washed by water (10 mL, 3 times), and then dried in oven. A Waters Associates Chromatograph (Model 6000A pump) was equipped with three columns, one Polymer Laboratories Mixed-C and two American Polymer Standard 100 in series, connected to the Shodex RI-71 refractive index detector. THF was used as the eluent and the flow rate was set as 1 mL/min. The average molecular weights of polymers were determined from the calibration curve established by means of polystyrene (PS) standards.

RESULTS AND DISCUSSION

All the experimental conditions in the following discussion are listed in Table III.

Conversion and rate of polymerization (R_p)

Curves of conversion versus time for different experimental conditions are shown in Figure 1. With eq. (5), the rate of polymerization can be calculated from the experimental curves of conversion versus time.

Figure 2 shows that in the emulsion polymerization, the rate of polymerization would be higher with lower concentration of MMA. The dome shape of the curve was a result of the gel effect; the less the monomer concentration, the earlier the maximum point appeared.

Similarly, from the curves of R_p versus time, it was found that the greater the amount of the ferrofluid, the faster is the polymerization rate. However, when the ferrofluid was more than 100 mL, there was no significant difference in the polymerization rate.

Also, as expected, the rate of polymerization was higher under the conditions of higher initiator concentration.

The morphology of composite polymer particles

Figure 3(a) shows the morphology of polymer particles of sample M15 at conversion of 91.80%. As the figures indicate, the magnetite was well encapsulated in polymer. The polymer particles of M15 were generated from seeds and it was a seeded emulsion polymerization, and so our modeling equation considered only eq. (1). Figure 3(b) shows the morphology of polymer particles of sample M30 at conversion of 90.84%. Some particles did not contain Fe_3O_4. The polymer particles of M30 were mostly generated from seeds and partially from self-nucleation. The other cases in this work showed similar morphology as M30. This meant that most of the particles encapsulated Fe_3O_4, but some particles did not contain Fe_3O_4,

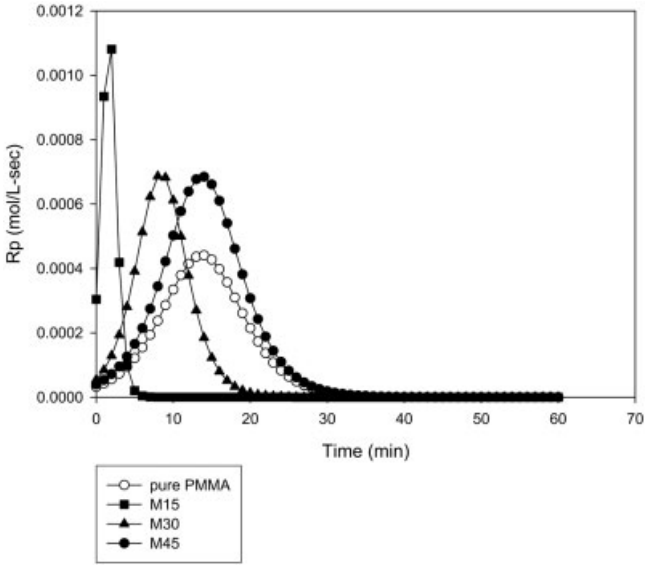

Figure 2 Rate of polymerization versus time at different monomer concentrations.

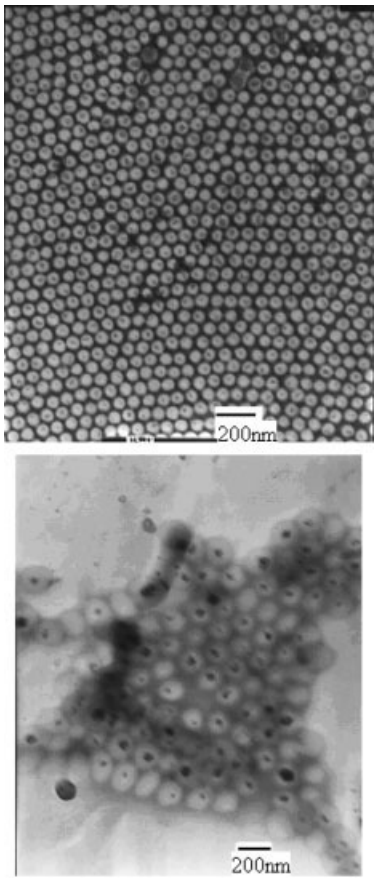

Figure 3 TEM photographs of sample (a) M15 at conversion of 91.80% and (b) M30 at conversion of 90.84%.

and so our modeling equations considered eqs. (1) and (2) simultaneously.

Concentration of polymer particles (*N*)

The number average diameter ($\bar{D}$) of polymer particles was obtained by measurement using a transmission electron microscope (TEM).[18] Then the experimental concentration of particles (N) was calculated by eq. (7). The results are shown in Figures 4–6 as point symbols. The particles of the samples of M45 and 0.5FD were not considered because the magnetic particles in these two samples coagulated seriously and influenced the results of the calculation.

Monomer concentration effect

Figure 4 shows the particle concentration versus conversion at different monomer concentrations. It indicates that the higher the monomer concentration, the less is the particle concentration. The sample of M15 was mostly synthesized by seeded polymerization. The particle concentration kept constant during the course of polymerization. The extent of coagulation was very small. In the system of M30, the particle

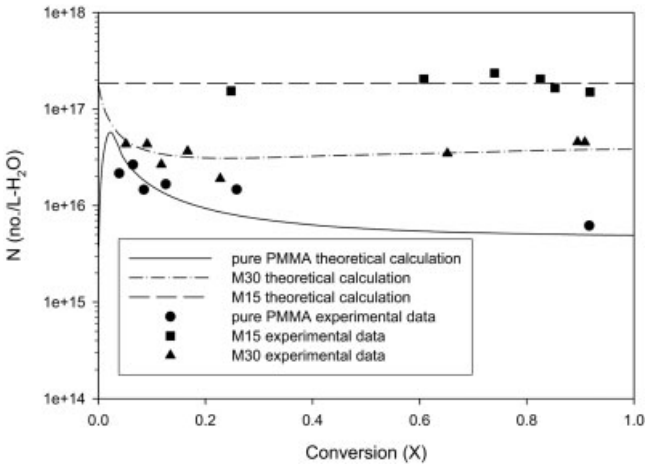

Figure 4 Concentration of composite polymer particles *versus* conversion at different monomer concentrations.

concentration dropped first and then slightly increased. Micelle nucleation occurred and caused the particle concentration to increase. For the pure PMMA system, there was a marked decrease in the particle concentration with the increasing conversion. After initial homogeneous nucleation, the coagulation occurred continuously during polymerization, and hence the concentration of the particles decreased.

Ferrofluid concentration effect

Particle concentration versus conversion, at different ferrofluid concentrations, is shown in Figure 5. As the figure indicates, the particle concentration of 2FD was lower than that of 1FD. The reason might be that the bilayer structure of surfactant in ferrofluid was unsta-

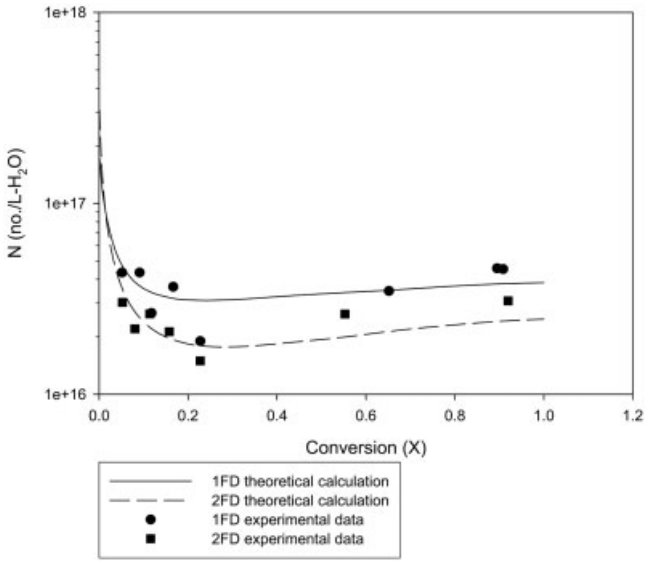

Figure 5 Concentration of composite polymer particles versus conversion at different ferrofluid concentrations.

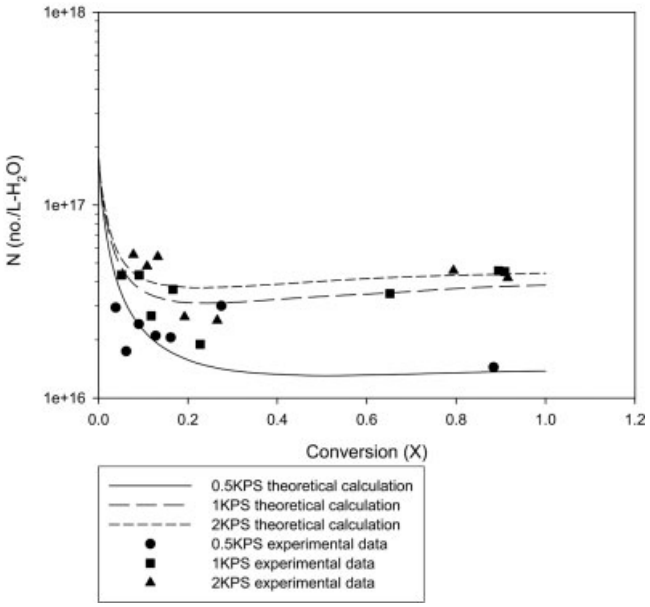

Figure 6 Concentration of composite polymer particles versus conversion at different initiator concentrations.

ble, and the greater the particle concentration of ferrofluid, the larger is the coagulation.

Initiator concentration effect

Figure 6 shows the particle concentration versus conversion at different initiator concentrations. The concentration of particles for 2KPS and 1KPS was almost the same because both systems followed mostly seeded polymerization and partially self-nucleation polymerization, and so the concentration of KPS had no significant influence on particle concentration. But for the case of 0.5KPS, the particle concentration decreased obviously. Because the lesser amount of SO_4^- charge (which came from KPS) on the surface of the latex particles decreased the repulsion force among particles, the lower surface charge density caused the larger extent of coagulation.

Simulation of concentration of polymer particles

In eq. (4), parameters a and b were adjustable constants (Table II). Other parameters needed in calculation are given in Table I. If the Runge-Kutta fourth-order method was selected, the concentration profile of composite polymer particles at different conditions could be simulated by eqs. (1)–(3). The results of simulation are shown in Figures 4–6. Compared with the experimental data of particle concentration, the theoretically simulated curves conformed well with the experimental data.

Average number of radicals per polymer particle

Once the calculation of R_p and N was completed, together with the equation of $[M_p]$(Table I), $\bar{n}$ could then be calculated by eq. (5). The results are described in Figure 7. When the conversion became higher, the gel effect gradually became more serious and lessened the probability of polymer radicals toward termination. Therefore, $\bar{n}$ increased quickly as the conversion was greater. This result also coincided with ESR's study.[21,23,24]

Monomer concentration effect

Comparing the curves of M15, M30 and pure PMMA in Figure 7, the $\bar{n}$ value was in the order of M15 $<$ M30 $<$ pure PMMA. The reason was due to the size of particles and the corresponding gel effect. The particle size of the pure PMMA system was larger than that of the systems with ferrofluid, so the diffusion effect (or gel effect) at high conversion was more significant. As a result, the $\bar{n}$ value was the largest for pure MMA system and $\bar{n}$ was the lowest for M15.

Ferrofluid concentration effect

Comparing the curves of 1FD and 2FD in Figure 7, the $\bar{n}$ value was in the order of 1FD $<$ 2FD. Because the particle size of 2FD was larger than that of 1FD, the $\bar{n}$ value of 2FD was larger than that of 1FD.

Initiator concentration effect

Comparing the curves of 0.5KPS, 1KPS, and 2KPS in Figure 7, the $\bar{n}$ value was in the order of 0.5KPS

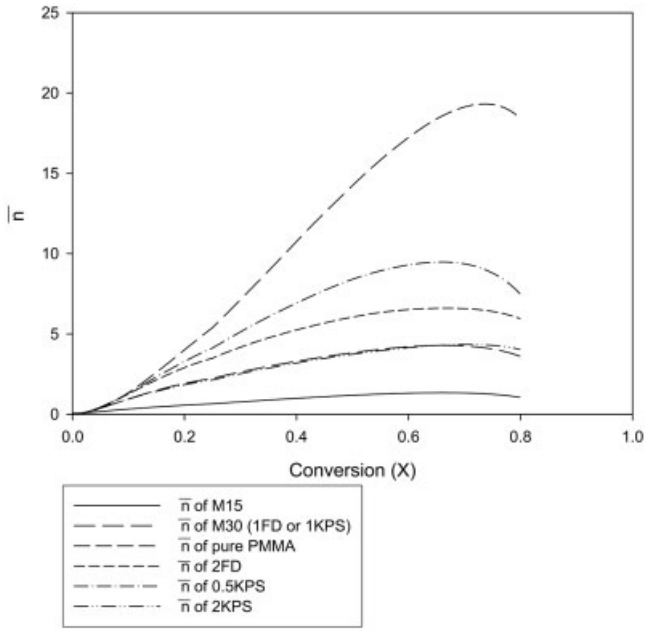

Figure 7 Average number of radicals per polymer particle versus conversion at different monomer concentrations.

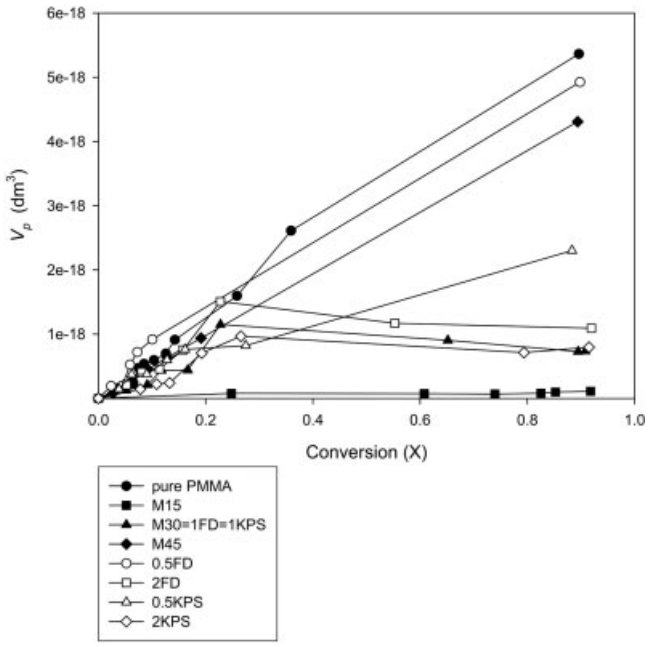

Figure 8 Volume of a swollen polymer particle *versus* conversion.

$>$ 1KPS≈2KPS. The particle size of 0.5KPS was larger than that of 1KPS or 2KPS, and so the $\bar{n}$ value of 0.5KPS was larger.

Volume of a swollen polymer particle

Under different experimental conditions, the variation of V_p during the reaction could be calculated using eqs. (9) and (10). This is shown in Figure 8.

Monomer concentration effect

M15 composite polymer latex was mostly synthesized by seeded polymerization. The V_p value slowly increased up to about 1.12×10^{-19} (dm^3) with increasing conversion. The coagulation between particles was almost negligible. In the system of M30, more monomer was present in the emulsion; the V_p value was larger than M15 as expected. As for the sample of M45, the ferrofluid bilayer structure was destroyed by the excess monomer, and the latex polymer particles were mostly generated through self-nucleation. So, the curve of M45 was very similar to the curve of pure PMMA. There was a marked increase in the V_p with increasing conversion. It indicated self-nucleation for the system of M45.

Ferrofluid concentration effect

Comparing the curves of different ferrofluid concentrations, the V_p versus conversion was similar in the cases of 1FD and 2FD. Both systems were mostly through seeded emulsion polymerization and partially from self-nucleation. But V_p versus conversion curve of 0.5FD had a different shape, analogous to M45, where particles were mainly generated through self-nucleation.

Initiator concentration effect

As for the cases of different initiator concentrations, the V_p value in both 1KPS and 2KPS cases were almost the same. But the V_p of 0.5KPS value was larger and kept going up at high conversion, because the latex particles had not enough surface charge SO_4^- from initiator to prevent coagulation.

Average molecular weight of polymers

Figure 9 shows the GPC curves at different experimental conditions. Two peaks were observed in most of the systems (except M15). The higher molecular weight peak was attributed to the diffusion effect during polymerization. The calculated average molecular weight and polydispersity of polymers from GPC curves are shown in Table IV.

Monomer concentration effect

The average molecular weight of polymers was in the order of M15 $<$ M30 $<$ M45 $<$ pure PMMA. It was due to the extent of gel effect. When the particles were smaller in size, the lower diffusion effect was observed, as reflected in the GPC curves.

Ferrofluid concentration effect

The average molecular weight of polymers was in the order of 1FD $<$ 2FD $<$ 0.5FD. It could also be explained by the extent of diffusion effect. The larger the

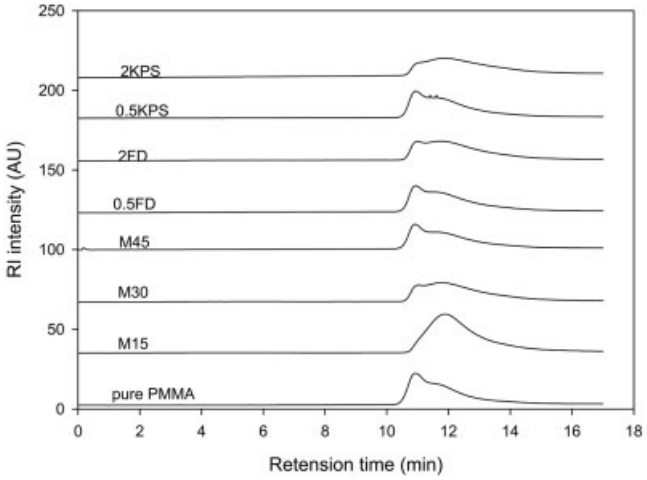

Figure 9 GPC curves at different experimental conditions.

TABLE IV
Average Molecular Weight and Polydispersity of Polymers from GPC

	M_n	M_w	PDI
Monomer effect			
Pure PMMA	83,500	248,900	2.98
M45	71,800	219,900	3.06
M30	49,800	147,800	2.97
M15	47,100	112,200	2.38
Initiator effect			
0.5KPS	71,800	211,900	2.95
1KPS	49,800	147,800	2.97
2KPS	37,400	123,900	3.31
Ferrofluid effect			
0.5FD	57,000	201,800	3.54
1FD	49,800	147,800	2.97
2FD	53,800	159,600	2.97

value of $\bar{n}$, the larger is the diffusion effect, and therefore, the average molecular weight of polymers increased.

Initiator concentration effect

The average molecular weight of polymers was in the order of 0.5KPS > 1KPS > 2KPS; the larger the concentration of initiator, the smaller is the average molecular weight as expected.

To make sure of the diffusion effect for the higher molecular weight peak of GPC curves shown in Figure 9, GPC curves of pure PMMA at different reaction times were measured. Only one peak was observed when conversion was low ($x < x_c$). A second peak with larger molecular weight appeared when conversion increased ($x \geq x_c$). For the PMMA system, the critical conversion x_c (at which monomer droplets disappeared) was about 0.25.[20] When $x < x_c$, the monomer in particles kept saturated concentration, and only one peak was observed. The diffusion effect was not important. When $x \geq x_c$, the monomer concentration in particles decreased gradually, the viscosity in particles increased, and the termination between polymer radicals was difficult. As a result, the diffusion effect was more and more obvious at high conversion.

Figure 10 shows the variation of $\overline{M_n}$ with conversion for pure PMMA. When $x < x_c$, the molecular weight was smaller. When $x \geq x_c$, because of the appearance of the larger molecular weight peak, the number average molecular weight was larger.

As also seen in Figure 10, for the ferrofluid system, the $\overline{M_n}$ of polymers at the end of the reaction was always lower than the $\overline{M_n}$ of pure PMMA system. The different extent of gel effect at different experimental conditions explained the results.

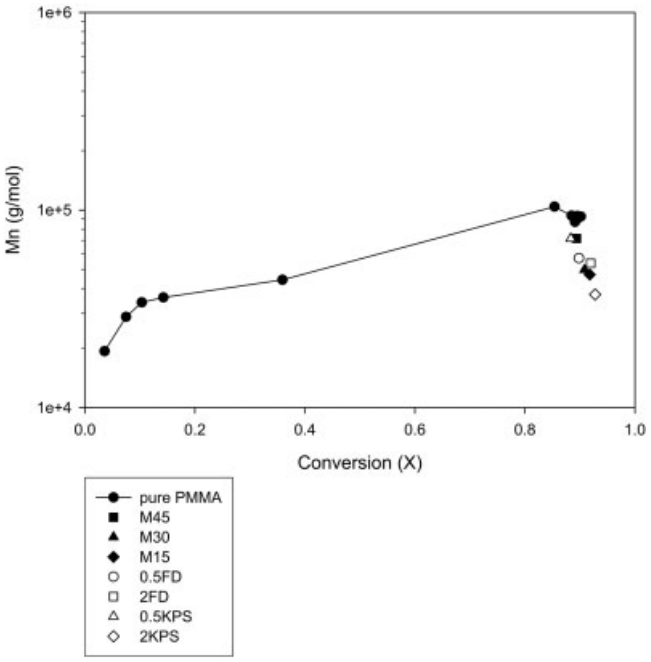

Figure 10 Number average molecular weight of polymers versus conversion.

Termination rate constant (k_t)

Combining the values of R_p, $\bar{n}$, V_p, and $\overline{M_n}$, the termination rate constant (k_t) could be calculated from eq. (11). The result is described in Figure 11. For pure PMMA, when $x < x_c$, the value of k_t ranges from 3.0×10^6 to 6.0×10^6 (L/mol s), close to the values reported in other references.[20] But when $x \geq x_c$, k_t decreased significantly with conversion due to the gel effect. The k_t value of the system with ferrofluid was

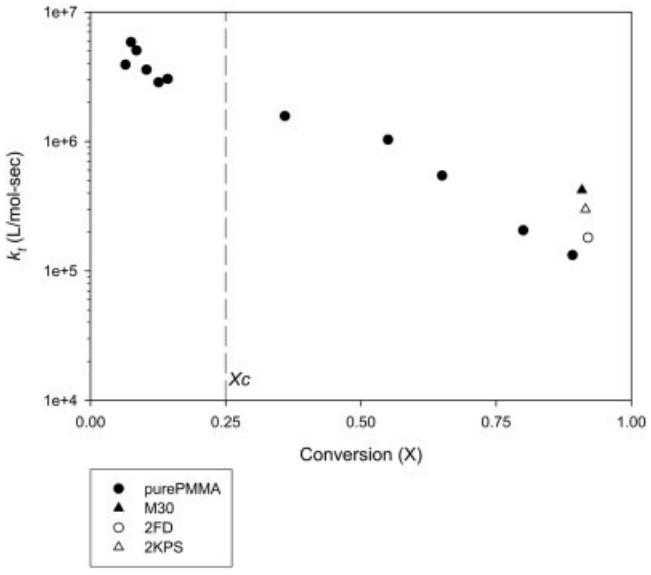

Figure 11 Termination rate constant versus conversion.

also calculated and is also shown in Figure 11 for comparison. The higher k_t values for the systems M30, 2FD, and 2KPS indicate the lesser extent of gel effect. This result is in agreement with the data of $\overline{M}_n$ and $\bar{n}$, as discussed earlier.

CONCLUSIONS

In this work, a combination of seeded nucleation, homogeneous nucleation, and micelle nucleation was considered to simulate the concentration of polymer particles under different experimental conditions for soapless emulsion polymerization of MMA with ferrofluid. The simulation results conformed well with the experimental data. From the calculation of particle concentration, the coagulation rate constant k_f with the conversion (x) was also obtained. The average number of radicals per polymer particle ($\bar{n}$) increased with increasing conversion (x), which infers that a gel effect was obvious with increasing conversion. For the pure PMMA system, the $\bar{n}$ value was the largest. For the case containing ferrofluid, the particle size was smaller and the $\bar{n}$ value was smaller, and so the gel effect was reduced. From the variation of $\overline{M}_n$ (number average molecular weight of polymers) with conversion in GPC curves, the gel effect occurred at $x \geq x_c$ (x_c: monomer droplets disappeared), which was reflected in the variation of termination rate constant k_t with conversion during the reaction.

References

1. Piirma, I. Emulsion Polymerization; Academic Press: New York, 1982.
2. Madaeni, S. S.; Ghanbarian, M. Polym Int 2000, 49, 1356.
3. Goodall, A. R.; Wilkinson, M. C.; Hearn, J. J Polym Sci Polym Chem Ed 1977, 15, 2193.
4. Cox, R. A.; Wilkinson, M. C.; Creasey, J. M.; Goodall, A. R.; Hearn, J. J Polym Sci Polym Chem Ed 1977, 15, 2311.
5. Chen, C. Y.; Piirma, I. J Polym Sci Polym Chem Ed 1980, 18, 1979.
6. Vanderhoff, J. W. J Polym Sci Polym Symp 1985, 72, 161.
7. Priest, W. J. J Phys Chem 1952, 56, 1077.
8. Fitch, R. M.; Tsai, C. H. Polymer Colloids; Plenum: New York, 1971; p 73.
9. Fitch, R. M. Br Polym J 1973, 5, 467.
10. Hansen, F. K.; Ugelstad, J. J Polym Sci Polym Chem Ed 1978, 16, 1953.
11. Hansen, F. K.; Ugelstad, J. J Polym Sci Polym Chem Ed 1979, 17, 3033.
12. Hansen, F. K.; Ugelstad, J. J Polym Sci Polym Chem Ed 1979, 17, 3047.
13. Ugelstad, J; Hansen, F. K. Rubber Chem Tech 1976, 49, 536.
14. Hansen, F. K.; Ugelstad, J. Emulsion Polymerization; Academic Press: New York, 1982; p 51.
15. Lee, C.-F.; Chiu, W.-Y.; Chern, Y.-C. J Appl Polym Sci 1995, 57, 591.
16. Lee, C.-F.; Chiu, W.-Y. J Appl Polym Sci 1995, 56, 1263.
17. Lee, C.-F.; Chiu, W.-Y. J Appl Polym Sci 1997, 65, 425.
18. Wang, P. C.; Chiu, W. Y.; Lee, C. F.; Young, T. H. J Polym Sci Part A: Polym Chem 2004, 42, 5695.
19. Chen, Y.-C. Institute of Materials Science and Engineering; National Taiwan University, Taiwan, 1993.
20. Chen, Y.-C.; Lee, C.-F.; Chiu, W.-Y. J Appl Polym Sci 1996, 61, 2235.
21. Song, Z.; Poehlein, G. W. J Colloid Interface Sci 1989, 128, 486.
22. Song, Z.; Poehlein, G. W. J Polym Sci Part A: Polym Chem 1990, 28, 2359.
23. Garrett, R. W.; Hill, D. J. T.; O'Donnell, J. H.; Pomery, P. J.; Winzor, C. L. Polym Bull (Berlin) 1989, 22, 611.
24. Zhu, S.; Tian, Y.; Hamielec, A. E.; Eaton, D. R. Macromolecules 1990, 23, 1144.